Front. Optoelectron. 2019, 12(2): 197–207
https://doi.org/10.1007/s12200-018-0838-5

RESEARCH ARTICLE

Saturation in wavelength-division multiplexing free-space optical communication systems

Jeremiah O. BANDELE (✉)[1*], Malcolm WOOLFSON[2], Andrew J. PHILLIPS[2*]

1 Department of Electrical, Electronics and Computer Engineering, College of Engineering, Afe Babalola University, Ado-Ekiti, Ekiti State, P.M.B 5454, Nigeria
2 Department of Electrical and Electronic Engineering, Faculty of Engineering, University of Nottingham, University Park, Nottingham, NG7 2RD, UK

Abstract The performance of a wavelength-division multiplexing (WDM) free-space optical (FSO) communication system in a turbulent atmosphere employing optical amplifiers to improve capacity is investigated, in the presence of amplified spontaneous emission noise, scintillation, beam spreading, atmospheric attenuation and interchannel crosstalk. Using on-off keying modulation, Monte Carlo simulation techniques are used to obtain the average bit error rate and system capability due to scintillation and the effect of introducing a power control algorithm (PCA) to the system is investigated. The PCA ensures that at any receiving instant, the same turbulence-free powers are received by all the receiving lenses. The performance of various WDM FSO communication system configurations such as non-amplified systems with an adaptive decision threshold (NOAADT), non-amplified systems with a non-adaptive decision threshold, fixed gain amplified systems with an adaptive decision threshold, fixed gain amplified systems with a non-adaptive decision threshold and saturated gain amplified systems with a non-adaptive decision threshold (SOANADT) are investigated. Results obtained show that the SOANADT is superior to the NOAADT and the PCA is only beneficial in amplified systems.

Keywords wavelength-division multiplexing (WDM), free-space optical (FSO) communication, crosstalk, optical amplifier (OA), gain saturation, decision threshold

Received May 30, 2018; accepted July 18, 2018

E-mail: jbandele@abuad.edu.ng

*was with Department of Electrical and Electronic Engineering, Faculty of Engineering, University of Nottingham, University Park, Nottingham, NG7 2RD, UK

1 Introduction

The growing popularity of the internet and the need for the simultaneous use of network services by multiple subscribers has brought about the need for network providers to provide high and stable bandwidths across multiple channels [1,2]. To satisfy this increasing demand for data usage, technologies based on optical communications (such as passive optical networks (PONs)) have been proposed due to the advantages they offer over radio frequency based communication systems such as high speeds and large bandwidths [3]. A variant of the PON, the wavelength-division multiplexing (WDM) PON; where each subscriber is assigned a different channel/wavelength, is seen as the most promising choice for a reliable access network [4]. A WDM PON has attributes such as high security, sufficient capacity (able to satisfy bandwidth demands) and being easily upgradeable but its high equipment cost and complicated operation (especially in the access network) makes its practical deployment problematic. Methods involving the use of low-cost transmitters have been proposed to alleviate this problem [5–7]. To realize multiplexing and demultiplexing in WDM systems, it is common to use devices based on arrayed waveguide grating (AWG) due to their low chromatic dispersion. However, due to the cost and intricacy of AWG-based devices, other multiplexing techniques such as free-space diffraction-grating have been proposed [8].

Optical fiber communication links (combined with dense WDM) have been used to obtain transmission speeds greater than 1 Tb/s (in the network core) but the high setup cost of fiber in the access region and lack of flexibility is currently diverting attention to free-space optical (FSO) communication systems. FSO communication systems are increasingly gaining recognition due to

the advantages they offer such as low cost, simplicity, immunity to electromagnetic interference, flexibility and no licensing requirements [3,9–11]. Thermal inhomogeneity, due to refractive index changes in the atmosphere, results in atmospheric turbulence [11,12] which causes fluctuations in the transmitted optical signal power and negatively affects the performance of FSO communication systems [11,13]. The effect of atmospheric turbulence becomes even more severe in long distance communication [14,15].

An optical amplifier (OA) has the ability to adjust its gain to new power levels by providing higher gains to lower input powers and lower gain to higher input powers [16]. This attribute of the OA has been shown in an earlier work to improve the system bit error rate (BER) in a turbulent atmosphere with unknown channel state information when a non-adaptive decision threshold is used at the receiver [16]. OAs can naturally be integrated with WDM systems since a single OA can concurrently amplify signals at different wavelengths within the gain region [17]. In choosing a gain flat (at least in the small signal regime) OA for FSO communication system, it is important to ensure the gain dynamics are fast enough to track fluctuations in the atmosphere. While the gain dynamics in both erbium-doped fiber amplifiers (EDFAs) and semiconductor OAs (SOAs) are fast enough to track the atmospheric turbulence fluctuations, EDFAs are preferable for WDM systems since they do not introduce gain crosstalk (from cross-gain modulation) into the system. Furthermore to continue to benefit from the turbulence mitigation, while avoiding gain crosstalk, it is necessary to ensure that individual channels saturate independently. This will be harder to achieve with an SOA than with an EDFA [18–20]. Crosstalk occurs in communication systems either due to optical component imperfections or power transmission between different channels caused by nonlinear effects [21]. It is particularly common in WDM networks due to the presence of multiple wavelengths and the effect is further exacerbated in FSO communication systems due to atmospheric turbulence [22]. In the upstream of WDM FSO communication systems, where the desired and crosstalk signals are assumed to follow independent paths, the fluctuations caused by atmospheric turbulence in both the desired and crosstalk signals poses a major limitation to system performance [8].

In Ref. [23], a 32×10 Gbps WDM FSO link limited by snow and rain weather was proposed and compared with existing WDM FSO links while a WDM FSO link employing multibeam and single beam technologies were compared in Ref. [24] under hazy and clear weather conditions. The power efficiency of different single-line and mixed-line rates were compared in Ref. [25] where an investigation was also carried out to ascertain the trade-off between power and spectral efficiency in a WDM network. In Ref. [26], the performance of M-ary quadrature amplitude modulation WDM FSO link limited by atmospheric turbulence and optical nonlinearity was studied and a WDM FSO link employing optical amplifiers (with hybrid arrangement) is shown in Ref. [27] to improve and increase the received signal power and maximum achievable link length respectively. The impact of interchannel crosstalk in non-amplified and amplified FSO communication systems was investigated in Refs. [8,28]. In Ref. [8] where the on–off keying (OOK) modulation format was used, an adaptive decision thresholding scheme was assumed at the receiver and the OAs used in Refs. [8] and [28] were only operated in the unsaturated gain regime. In this paper, a direct detection scheme with non-return-to-zero OOK modulation is considered and a Monte Carlo (MC) simulation approach is also used to analyze the upstream of WDM FSO communication systems using adaptive and non-adaptive decision thresholding schemes. For amplified systems, results are obtained for instances where the OA gains are either in the fixed or saturated gain regimes. Additionally, results are also shown for instances where a power control algorithm (PCA) ensures that at any receiving instant, the same turbulence-free powers (equal to the power received from the farthest transmitter) are received by both receiving lenses. In a more general sense (i.e., for any WDM system where it is assumed that all the receiving lenses are situated at the same location), the PCA is actualised by turning down the powers of all the transmitters (except the farthest transmitter; which is used as reference).

After this introductory part, the statistical model used to describe atmospheric turbulence-induced fading in the WDM FSO communication system is described in Section 2. Section 3 describes the upstream transmission of a WDM FSO communication system. Section 4 describes the WDM FSO communication system modeling and BER analysis. The results of the MC simulations for the WDM FSO communication system are presented in Section 5 and a conclusion is provided in Section 6.

2 Channel statistics

Various statistical models have been used to describe atmospheric turbulence-induced fading [29]. The lognormal (LN) distribution is commonly used to characterize the weak turbulence regime [30,31] and its probability density function is given as [11]

$$f_{LN_h}(h)=\frac{1}{h\sqrt{2\pi\sigma_l^2}}\exp\left\{-\frac{\left[\ln(h)+\frac{1}{2}\sigma_l^2\right]^2}{2\sigma_l^2}\right\}, \quad (1)$$

where h represents the parameter used to describe the varying atmospheric turbulence-induced channel gain (or loss). The variance of the natural logarithm of the

irradiance is given as [11]

$$\sigma_l^2 = \exp\left[\frac{0.49\sigma_R^2}{(1+1.11\sigma_R^{12/5})^{7/6}} + \frac{0.51\sigma_R^2}{(1+0.69\sigma_R^{12/5})^{5/6}}\right] - 1, \quad (2)$$

where σ_R^2 represents the Rytov variance used to characterize the different atmospheric turbulence regimes and it is given as [29]

$$\sigma_R^2 = 1.23 C_n^2 k^{7/6} D^{11/6}, \quad (3)$$

where C_n^2 represents the refractive index structure parameter, D represents the length of the FSO link and $k = 2\pi/\lambda$ represents the optical wave number where λ represents the optical wavelength.

3 System configuration

A practical WDM FSO system is made up of many wavelengths, and signals on each wavelength is limited by the contribution of crosstalk from signals on all other wavelengths. It is however noteworthy that crosstalk effects from adjacent wavelengths are more critical than those from further separated wavelengths. Therefore, two WDM channels are considered in this paper to generate the fundamental understanding of how such a system operates and can be modeled. Clearly the multi-wavelength case is more complex but basic understanding of how it will work can come from this underpinning. Note that a single crosstalk channel (two WDM channels) is applicable where a worst-case performance analysis (combining multiple crosstalk signals into a single wavelength and modeling such as a single crosstalk) is carried out. Figure 1 shows a WDM FSO communication system model where both TX 1 and TX 2 can transmit either desired or crosstalk signals (with the two wavelengths assumed to have a channel spacing of 100 GHz on the ITU-T grid [32]). This means that at RX 1, TX1 and TX 2 are seen as the desired and crosstalk transmitter respectively and at RX 2, TX 2 and TX 1 are seen as the desired and crosstalk transmitter respectively. In Fig. 1, both the desired and crosstalk signals are sent through lenses into the atmosphere. Note that while propagating through the atmospheric channel, the desired and crosstalk signal paths are assumed (with proper alignment) to be independent of each other such that they do not interact either in the atmosphere or at the receiving lenses. After both signals are collected by their respective receiving lenses (which are assumed to be at the same location, e.g., rooftop), they are multiplexed and amplified before onward transmission through a feeder fiber. At the receiving end, the signals are demultiplexed and received by their respective receivers. Interchannel crosstalk (the crosstalk type considered in this paper) is caused by imperfections in the demultiplexer and it is more severe in WDM FSO communication systems due to the fluctuations in the crosstalk signal [8,28].

4 System modeling and BER analysis

For computational convenience, a MC simulation technique is used to model the WDM FSO communication system. With the MC simulation approach, the BER analysis (with respect to the 'desired signal' receiver) is first carried out for a random sample after which averaging takes place over all the samples to obtain the average BER. By assuming that the desired and crosstalk signals (each transmitted with signal power P_{t_z} for $z \in \{sig, xt\}$) are propagated in a clear atmosphere, the total loss in the FSO link $L_z = L_{nt_z} h_{LN}$ where h_{LN} represents the LN random variable describing the fluctuations due to atmospheric turbulence and L_{nt_z}; which represents the turbulence-free fixed path loss (< 1) is given as [28]

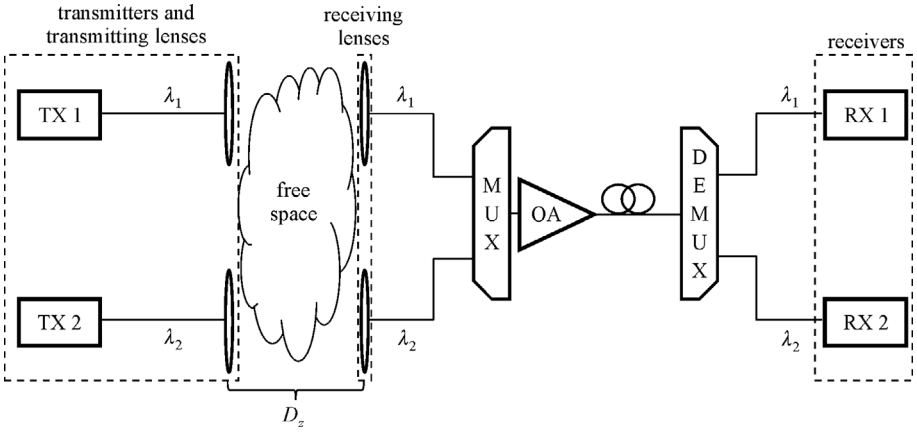

Fig. 1 A WDM FSO communication system (upstream transmission)

$$L_{nt_z} = \left(\frac{d_{rx_z}}{d_{bD_z}}\right)^2 \alpha_z, \tag{4}$$

where d_{rx_z} represents the receiving lens diameter and $d_{bD_z} = \phi_z D_z$ represents the beam diameter due to diffraction alone where ϕ_z represents the transmitter beam divergence angle. $\alpha_z = 10^{(-\alpha_{D_{fso_z}} D_z/10)}$ represents the atmospheric attenuation in the FSO link where $\alpha_{D_{fso_z}}$ represents the atmospheric attenuation factor. The signal power at the receiving lens $P_{lens_z} = P_{t_z} L_z$. The multiplexed signals are amplified by an OA with gain G and amplified spontaneous emission (ASE) power spectral density (PSD) $N_0 = 0.5(NFG-1)h\nu$, where NF is the noise figure, h is the Planck constant and ν is the frequency of the optical carrier. The instantaneous optical signal power at the OA input P_{in_z} is implicitly related to the OA gain G as shown below [22]

$$P_{in_z} = \frac{P_{sat}}{G-1} \ln\left(\frac{G_{ss}}{G}\right), \tag{5}$$

where P_{sat} and G_{ss} represents the internal saturation power and the small signal gain of the OA respectively. At the decision circuit, the mean desired signal current level at the sampling instant is given as

$$i_{sig_x} = RP_{r_{sig_x}} \ (x \in \{0,1\}), \tag{6}$$

where the desired signal power in a ONE $P_{r_{sig_1}} = [2r(P_{lens_{sig}} G L_{fibre})]/(r+1)$. $P_{lens_{sig}}$ represents the desired signal power at the input of the desired signal receiving lens ($Lens_{rx_{sig}}$), L_{fibre} represents the feeder fiber loss, r represents the extinction ratio and the desired signal power in a ZERO $P_{r_{sig_o}} = P_{r_{sig_1}}/r$. The responsivity $R = \eta q/h\nu$ where η is the quantum efficiency and q is the electronic charge. Also, the mean crosstalk signal current level at the sampling instant is given as

$$i_{xt_y} = RP_{r_{xt_y}} \ (y \in \{0,1\}), \tag{7}$$

where the crosstalk signal power in a ONE $P_{r_{xt_1}} = [2r(P_{lens_{xt}} G L_{fibre} L_{demux})]/(r+1)$, where $P_{lens_{xt}}$ represents the crosstalk signal power at the input of the crosstalk signal receiving lens ($Lens_{rx_{xt}}$), L_{demux} represents the extra loss experienced when the demultiplexer couples the crosstalk signal with the desired signal photodiode and the crosstalk signal power in a ZERO $P_{r_{xt_o}} = P_{r_{xt_1}}/r$. The total noise current variance is given as [8]

$$\sigma^2_{sig_x,xt_y} = \sigma^2_{sig_x,sp} + \sigma^2_{xt_y,sp} + \sigma^2_{sp,sp} + \sigma^2_{sh,sp} + \sigma^2_{sh_{sig_x,xt_y}} + \sigma^2_{th}, \tag{8}$$

where the signal-spontaneous beat noise is given as

$$\sigma^2_{sig_x,sp} = 4R^2 P_{r_{sig_x}} N_0 B_e, \tag{9}$$

where the receiver noise equivalent bandwidth, $B_e = 0.7R_b$ and R_b is the bit rate. The crosstalk-spontaneous beat noise is given as

$$\sigma^2_{xt_y,sp} = 4R^2 P_{r_{xt_y}} N_{0-xt} B_e, \tag{10}$$

where $N_{0-xt} = N_0 L_{demux}$ represents the ASE PSD at the signal receiver (but at or near the crosstalk wavelength). The spontaneous-spontaneous beat noise is given as

$$\sigma^2_{sp-sp} = 2m_t R^2 N_0^2 B_{opt} B_e \left(1 - \frac{B_e}{2B_{opt}}\right), \tag{11}$$

where m_t is the number of polarization states parameter and B_{opt} is the optical band pass filter (OBPF) bandwidth. The ASE shot noise is given as

$$\sigma^2_{sh-sp} = 2m_t qRN_0 B_{opt} B_e, \tag{12}$$

and the total shot noise (due to the desired and crosstalk signals) is given as

$$\sigma^2_{sh_{sig_x,xt_y}} = 2qR[(P_{r_{sig_x}} + P_{r_{xt_y}}) + m_t N_0 B_{opt}]B_e. \tag{13}$$

The instanteneous BER (i.e., obtained after a single MC iteration) is given as [16]

$$BER = \frac{1}{4}\left[\begin{array}{l} \frac{1}{2}\mathrm{erfc}\left(\frac{i_D - (i_{sig_0} + i_{xt_0})}{\sqrt{2\sigma^2_{sig_0,xt_0}}}\right) + \frac{1}{2}\mathrm{erfc}\left(\frac{i_D - (i_{sig_0} + i_{xt_1})}{\sqrt{2\sigma^2_{sig_0,xt_1}}}\right) \\ + \frac{1}{2}\mathrm{erfc}\left(\frac{(i_{sig_1} + i_{xt_0}) - i_D}{\sqrt{2\sigma^2_{sig_1,xt_0}}}\right) + \frac{1}{2}\mathrm{erfc}\left(\frac{(i_{sig_1} + i_{xt_1}) - i_D}{\sqrt{2\sigma^2_{sig_1,xt_1}}}\right) \end{array}\right], \tag{14}$$

where i_D represents the decision thresholding scheme used at the receiver. For an adaptive decision threshold, it is given as

$$i_D = \frac{\sigma_{sig_1,xt_0}(i_{sig_0} + i_{xt_1}) + \sigma_{sig_0,xt_1}(i_{sig_1} + i_{xt_0})}{\sigma_{sig_1,xt_0} + \sigma_{sig_0,xt_1}}, \tag{15}$$

and for a non-adaptive decision threshold (a fixed value equal to the long-term average of the desired and crosstalk signal powers), it is given as

$$i_D = \frac{R\sum_{n=1}^{N}(P_{sig_n} + P_{xt_n})}{N}, \tag{16}$$

where n represents the trials count, N represents the total number of trials used for the MC simulation, the desired signal power at the receiver $P_{sig_n} = P_{lens_{sig_n}} GL_{fibre}$ and the crosstalk signal power at the receiver $P_{xt_n} = P_{lens_{xt_n}} GL_{fibre}L_{demux}$. The average BER is then given as

$$BER_{ave} = \frac{\sum_{n=1}^{N} BER_n}{N}. \tag{17}$$

5 Results and discussion

The parameters used for the MC simulations are shown in Table 1. It is assumed that the saturated operation integrates the effect of ASE noise, responds freely and uses complete saturation characteristics. Also, a non-saturable OA ($P_{sat} \rightarrow \infty$) is called a fixed gain OA and a saturable OA (P_{sat} = 5 dBm) is called a saturated gain OA. A sensitivity of –23 dBm analogous to a BER of 10^{-12} is used to calculate the receiver thermal noise current (i.e., 7×10^{-7} A) [13]. Note that all the transmitters and receivers used in this analysis are assumed to have the same beam divergence angle and lens diameter respectively. The desired signal transmitting lens is assumed to be pointed directly at $Lens_{rx_{sig}}$ and the crosstalk signal transmitting lens is assumed to be pointed directly at $Lens_{rx_{xt}}$. For brevity sake, the desired signal is referred to as 'signal' and the crosstalk signal is referred to as 'crosstalk'. Results are obtained for the weak ($C_n^2 = 10^{-15}$ m$^{-2/3}$) turbulence regime.

Table 1 Parameters used for the simulations

parameter	symbol	value
desired signal wavelength	λ_{sig}	1550.12 nm
crosstalk signal wavelength	λ_{xt}	1550.92 nm
bit rate	R_b	2.5 Gb/s
OBPF bandwidth	B_{opt}	76 GHz
noise figure	NF	5 dB
quantum efficiency	η	0.8
extinction ratio	r	10 dB
transmitted optical power (maximum permitted)	P_t	10 dBm
OA small signal gain	G_{ss}	25 dB
feeder fiber length	D_{fibre}	20 km
feeder fiber loss	$\alpha_{D_{fibre}}$	0.2 dB/km
atmospheric channel loss	$\alpha_{D_{fso}}$	0.2 dB/km (clear air)
receiving lens diameter	d_{rx}	4 cm
beam divergence angle	ϕ	1 mrad

The WDM FSO communication systems considered includes non-amplified systems with an adaptive decision threshold (NOAADT), non-amplified systems with a non-adaptive decision threshold (NOANADT), fixed gain amplified systems with an adaptive decision threshold (FOAADT), fixed gain amplified systems with a non-adaptive decision threshold (FOANADT) and saturated gain amplified systems with a non-adaptive decision threshold (SOANADT).

In all cases considered, results are obtained for instances where $P_{lens_{sig}}$ and $P_{lens_{xt}}$ are only affected by L_{sig} and L_{xt} respectively. Since the feeder fiber length is assumed fixed, any reference to link lengths refers to the lengths of the FSO link. Note that D_{sig} and D_{xt} represents the length of the signal and crosstalk links relative to the positions of $Lens_{rx_{sig}}$ and $Lens_{rx_{xt}}$ (both at 0 km). For instance, longer D_{sig} and D_{xt} mean lower signal and crosstalk powers respectively.

Figure 2 shows the BER curves for different WDM FSO communication systems when L_{demux} = 15 dB. The BER curves are obtained for instances when $D_{sig} = D_{xt}$. In Fig. 2(a) where a PCA is not applied, the NOAADT, NOANADT, FOAADT, FOANADT and SOANADT are able to achieve a BER of 10^{-12} at 0.82 km, 0.6 km, > 2 km, 0.82 km and 0.87 km respectively. In Fig. 2(b) where a PCA is applied, the NOAADT, NOANADT, FOAADT, FOANADT and SOANADT are also able to achieve a BER of 10^{-12} at 0.82 km, 0.6 km, > 2 km, 0.8 km and 0.91 km respectively. As expected, Figs. 2(a) and 2(b) shows that the PCA has no significant impact on system performance when the signal and crosstalk link lengths are always equal.

Figure 3 shows the average BER values obtained without a PCA for different D_{sig} and D_{xt} when L_{demux} = 30 dB. The benefit of including an amplifier in a WDM FSO communication system is highlighted by comparing the systems with an adaptive decision threshold (i.e., NOAADT and FOAADT). In the FOAADT, a BER of less than 10^{-12} is attainable when D_{sig} and D_{xt} is 2 km compared to the NOAADT where BER values higher than 10^{-2} are obtained for the same link length. Also, a BER of less than 10^{-12} is always achievable with the FOAADT when D_{sig} and D_{xt} is about 2 km and more than 0.1 km respectively. This is a huge improvement on the NOAADT where BER values less than 10^{-12} can only always be achieved when D_{sig} is less than 0.5 km.

For the systems with a non-adaptive decision threshold (NOANADT, FOANADT and SOANADT), amplification

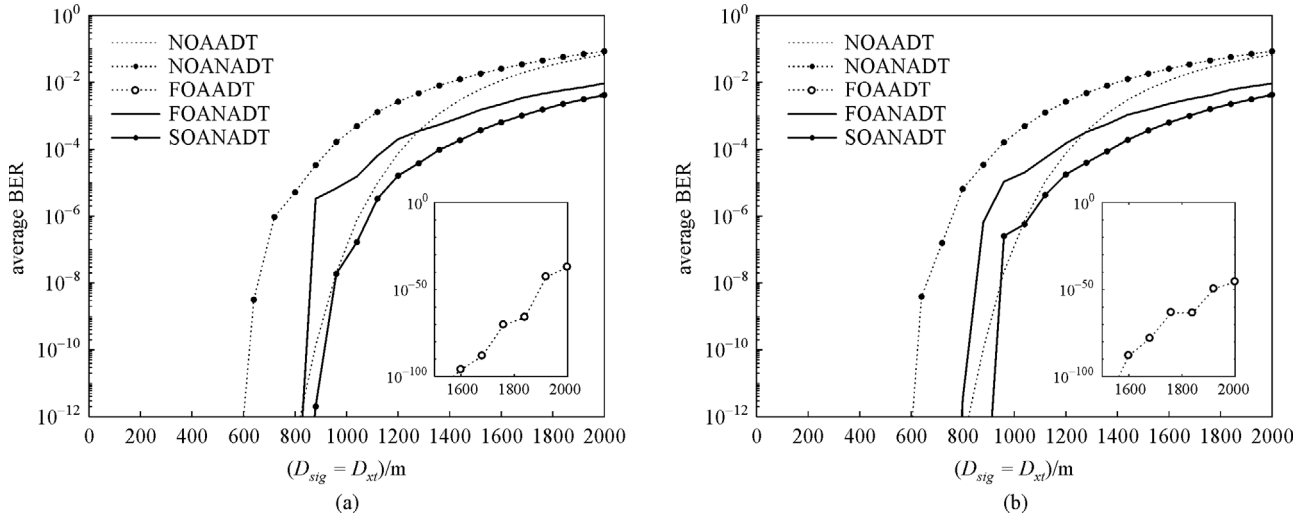

Fig. 2 Average BER against link length in WDM FSO communication systems (L_{demux} = 15 dB). (a) No PCA; (b) with PCA

is also advantageous and has more significant effect on system performance (especially for turbulence mitigation) when the OA is operated in the saturation regime. For instance, among the three systems, the longest link lengths achieving a BER of 10^{-12} (i.e., $D_{sig} \approx 1$ km and D_{xt} = 2 km) were obtained with the SOANADT. This shows the importance of using a saturated OA with a non-adaptive decision threshold. For any particular D_{sig}, the system performance is naturally expected to improve as D_{xt} increases (i.e., lower crosstalk power). However some instances in Fig. 3 show a reduction in system performance as D_{xt} increases. This can be attributed to an increase in atmospheric turbulence effects due to longer link lengths. In other words, while the crosstalk adversely affects the performance of WDM FSO communication systems, the system performance also largely depends on the turbulent state of the atmosphere.

Figures 4 shows the capability of various WDM FSO communication systems (with L_{demux} = 30 dB and target BER = 10^{-12}) when D_{sig} and D_{xt} are varied. In Fig. 4, 0 m indicates that the transmitter is placed just in front of the receiver and 2000 m indicates that the transmitter is placed at a distance of 2000 m from the receiver. Note that when D_{sig} = 0 m and D_{xt} = 2000 m, the crosstalk signal is almost negligible and when D_{sig} = 2000 m and D_{xt} = 0 m, the desired signal is almost negligible. Also, the shaded areas in Fig. 4 show the link lengths at which the target BER is met. In the NOAADT shown in Fig. 4(a) where a PCA is not applied, the target BER is met when $D_{sig} < 880$ m and $D_{xt} > 80$ m. When $D_{xt} < 80$ m, a $D_{sig} < 620$ m is required to achieve the target BER. When a PCA is applied in Fig. 4 (b), the target BER is met when $D_{sig} < 640$ m and $D_{xt} < 960$ m. While the target BER is also met at other link lengths ($D_{sig} < 880$ m and $D_{xt} < 880$ m) in Fig. 4(b), the target BER is not met when $D_{xt} > 1040$ m for all D_{sig} considered. This is because the PCA ensures that even when D_{sig} = 0 m (desired signal transmitter placed just in front of the receiver) and $D_{xt} > 1040$ m (crosstalk signal transmitter placed at a link length > 1040 m from the receiver), the received signal power is set to the received crosstalk power, leading to errors. In the NOANADT shown in Fig. 4(c) where a PCA is not applied, the target BER is met when $D_{sig} < 560$ m for all D_{xt} considered. As expected, this performance is lower than the NOAADT performance shown in Fig. 4(a) due to the non-adaptive decision threshold used in Fig. 4(c). When a PCA is applied in Fig. 4(d), the target BER is met when $D_{sig} < 400$ m and $D_{xt} < 880$ m. The target BER is also met at other link lengths ($D_{sig} < 120$ m and $D_{xt} < 960$ m). The errors observed in Fig. 4(b) due to the PCA are also observed in Fig. 4(d) where the target BER is not met when $D_{xt} > 960$ m for all D_{sig} considered. Compared to Fig. 4(a), the advantage of amplification is observed in the FOAADT shown in Fig. 4(e) where a PCA is not applied. In Fig. 4(e), the target BER is met when $D_{xt} > 160$ m for all D_{sig} considered. Also, when $D_{xt} < 80$ m, the target BER is met when $D_{sig} < 880$ m. In contrast to Figs. 4(b) and 4(d) where the PCA limited the system performance, the target BER is met for all D_{sig} and D_{xt} considered when a PCA is applied in Fig. 4(f). This shows that amplification is needed for the PCA to have a beneficial impact on system performance. In the FOANADT shown in Fig. 4(g) where a PCA is not applied, the target BER is met when $D_{sig} < 640$ m for all D_{xt} considered. Also, the target BER is met when $D_{sig} < 800$ m and $D_{xt} > 80$ m. When a PCA is applied in Fig. 4(h), the target BER is also met when $D_{sig} < 640$ m for all D_{xt} considered but compared to Fig. 4(g), Fig. 4(h) shows an increased performance when D_{xt} = 0 m and a reduced performance when D_{xt} = 2000 m. This means that the PCA becomes less beneficial with increased link lengths. The benefit of using a gain saturated amplifier for turbulence mitigation is observed in the

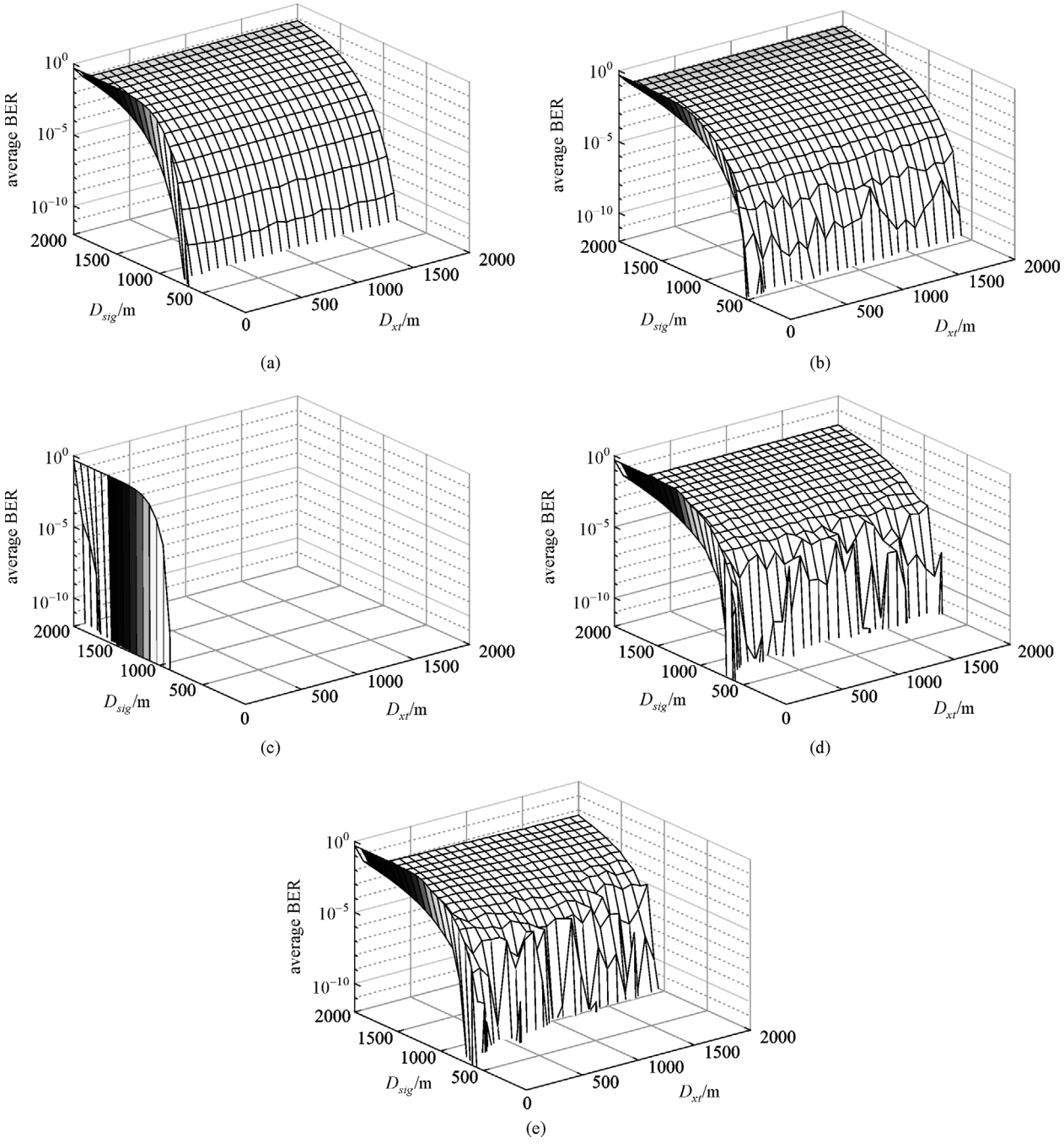

Fig. 3 Average BER at various link lengths for WDM FSO communication systems without a PCA (L_{demux} = 30 dB). (a) NOAADT; (b) NOANADT; (c) FOAADT; (d) FOANADT; (e) SOANADT

SOANADT shown in Fig. 4(i) where a PCA is not applied. Compared to the NOAADT (where the target BER is not met at $D_{sig} > 880$ m for all D_{xt} considered), improved system performance is observed in Fig. 4(i) where the target BER is met at D_{sig} = 1040 m and D_{xt} = 2000 m. When a PCA is applied in Fig. 4(j), an increased performance is observed at reduced D_{xt} and a reduced performance is noticed at increased D_{xt}. These results align with results in Fig. 4(h) and it further proves that while the PCA benefits amplified system, it would impair system performance with increased link lengths.

6 Conclusion

This paper examined the performance of a WDM FSO communication system in a turbulent atmosphere by applying MC simulation techniques. Results obtained in

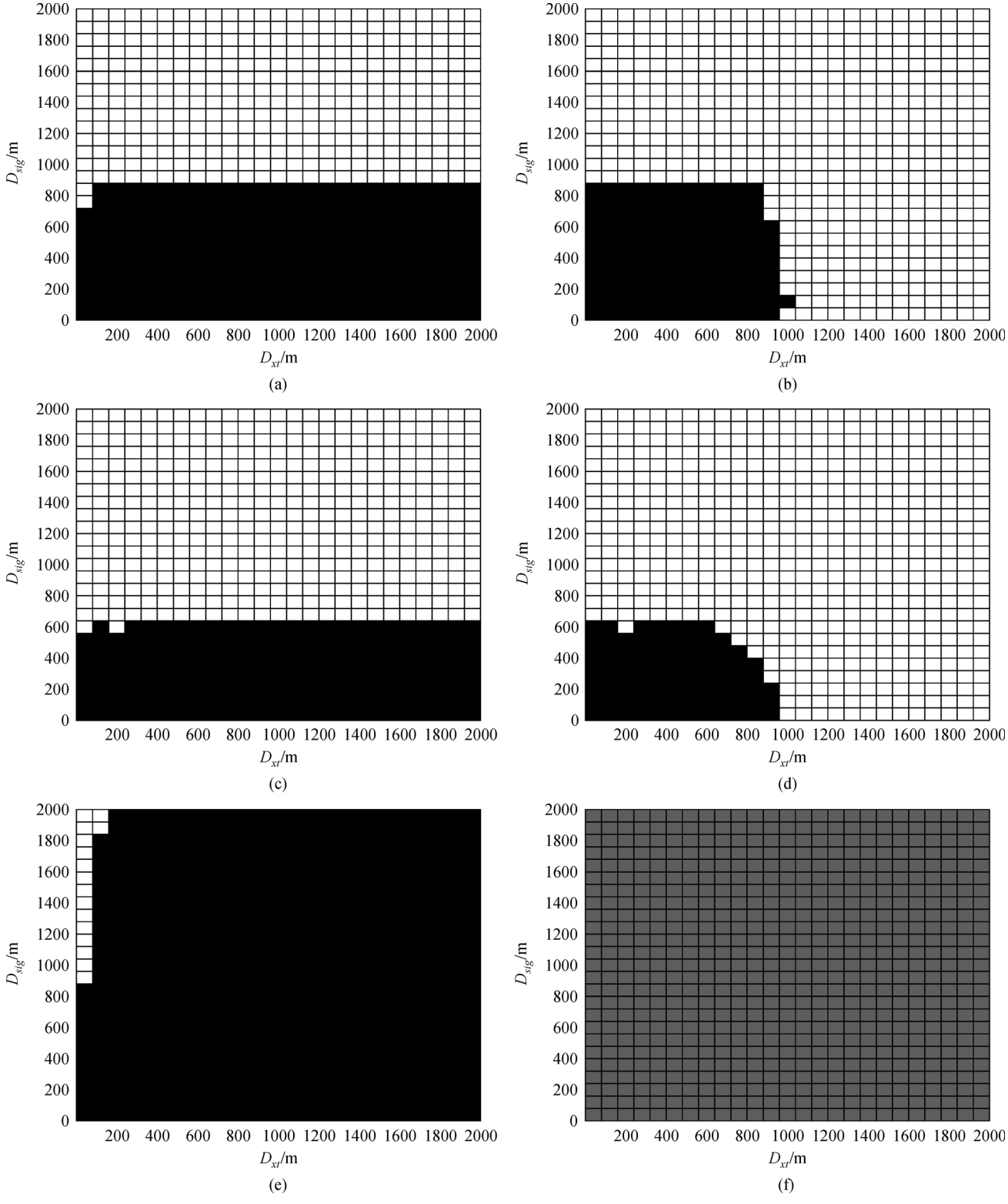
2000
1800
1600
1400
1200
1000
800
600
400
200
0
D_{sig}/m
200 400 600 800 1000 1200 1400 1600 1800 2000
D_{xt}/m
(a)
(b)
(c)
(d)
(e)
(f)

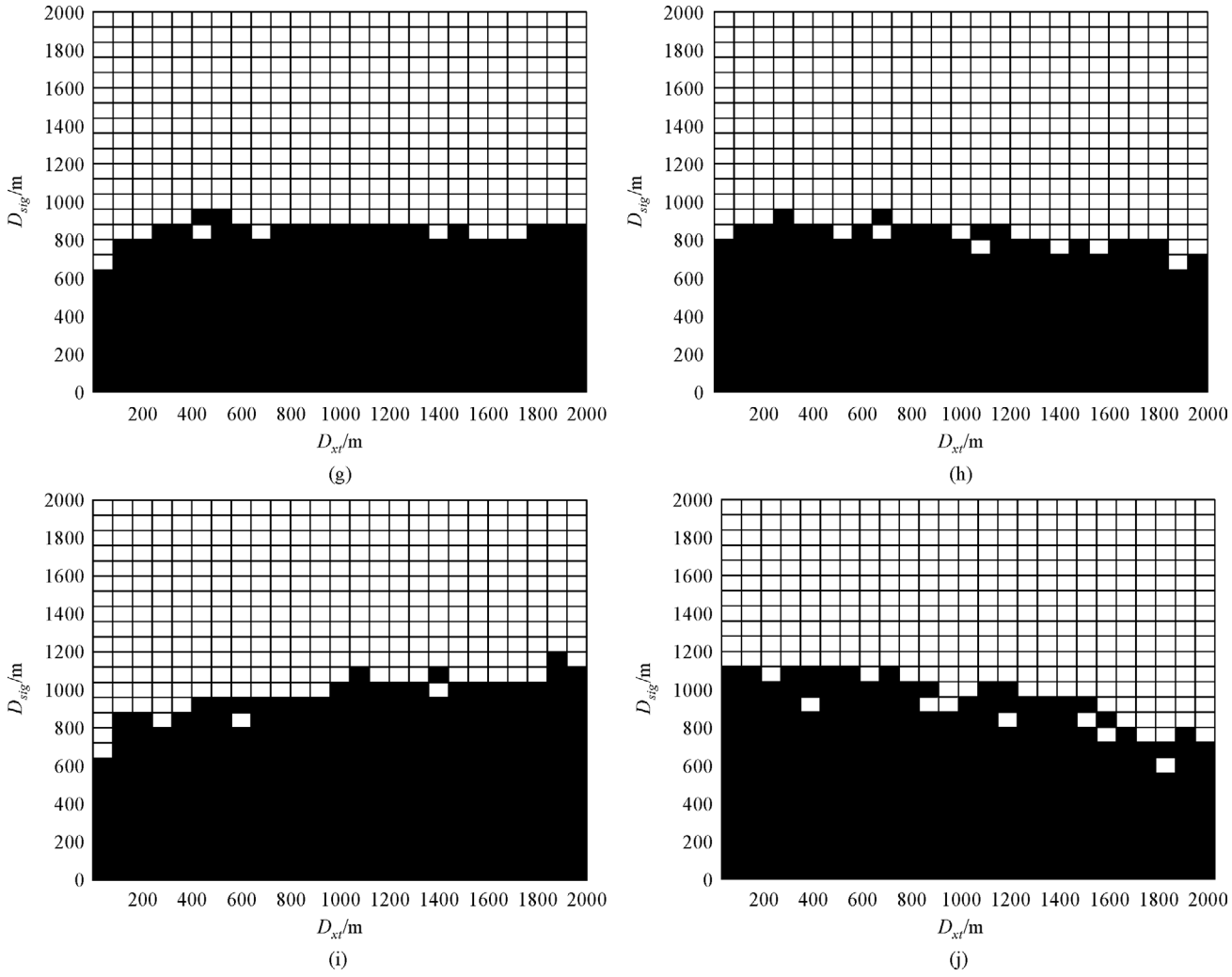

Fig. 4 Capability of WDM FSO communication systems (Ldemux = 30 dB and target BER = 10^{-12}). (a) NOAADT, no PCA; (b) NOAADT, with PCA; (c) NOANADT, no PCA;(d) NOANADT, with PCA; (e) FOAADT, no PCA; (f) FOAADT, with PCA; (g) FOANADT, no PCA; (h) FOANADT, with PCA; (i) SOANADT, no PCA; (j) SOANADT, with PCA

this paper showed that even when the crosstalk power is very small compared to the signal power, the fluctuations in the crosstalk due to atmospheric turbulence may have an adverse effect on system performance. Results obtained also show that amplification is needed for the PCA to have a beneficial impact on system performance. In fact, the PCA limits system performance in non-amplified systems. Also, the SOANADT performed better than the NOAADT. This is because the OA in the SOANADT is well driven into the saturation regime (due to the combination of the signal and crosstalk powers at the OA input) thereby elaborating the advantage of using a non-adaptive decision threshold. Lastly, even though the use of an adaptive decision threshold with optical amplification has once again proved to give the best results in FSO communication systems, the use of a saturated gain OA with a non-adaptive decision threshold has the capacity to provide acceptable performances for short distance communication (i.e., < 2 km) when the OA input power is high enough. However, care has to be taken not to overload the receiver.

References

1. Lee S M, Mun S G, Kim M H, Lee C H. Demonstration of a long-reach DWDM-PON for consolidation of metro and access networks. Journal of Lightwave Technology, 2007, 25(1): 271–276
2. Chandy R. Design of a reliable WDM-PON system with transmitter powered by a renewable energy source. In: Proceedings of 16th International Conference on Transparent Optical Networks (ICTON). 2014, 1–3
3. Ciaramella E, Arimoto Y, Contestabile G, Presi M, D'Errico A, Guarino V, Matsumoto M. 1.28 terabit/s (32 ×40 Gbit/s) WDM transmission system for free space optical communications. IEEE Journal on Selected Areas in Communications, 2009, 27(9): 1639–1645
4. Nguyen Q T, Bramerie L, Girault G, Vaudel O, Besnard P, Simon J

C, Shen A, Duan G H, Kazmierski C. 16 ×2.5 Gbit/s downstream transmission in colorless WDM-PON based on injection-locked fabry-perot laser diode using a single quantum dash mode-locked fabry-perot laser as multi-wavelength seeding source. In: Proceedings of Conference on Optical Fiber Communication (OFC). 2009, p.OThA3

5. Won Y Y, Kim H S, Son Y H, Han S K. Full colorless transmission of millimeter-wave band gigabit data over WDM-PON using sideband routing. In: Proceedings of Asia Communications and Photonics Conference and Exhibition (ACP). 2011, 1–8
6. Shin D J, Jung D K, Lee J K, Lee J H, Choi Y H, Bang Y C, Shin H S, Lee J, Hwang S T, Oh Y J. 155 Mbit/s transmission using ASE-injected Fabry-Perot laser diode in WDM-PON over 70°C temperature range. Electronics Letters, 2003, 39(18): 1331–1332
7. Mun S G, Cho H S, Lee C H. A cost-effective WDM-PON using a multiple section Fabry–Pérot laser diode. IEEE Photonics Technology Letters, 2011, 23(1): 3–5
8. Aladeloba A O, Woolfson M S, Phillips A J. WDM FSO network with turbulence-accentuated interchannel crosstalk. Journal of Optical Communications and Networking, 2013, 5(6): 641–651
9. Bock C, Prat J, Walker S D. Hybrid WDM/TDM PON using the AWG FSR and featuring centralized light generation and dynamic bandwidth allocation. Journal of Lightwave Technology, 2005, 23 (12): 3981–3988
10. Zhou H, Mao S, Agrawal P. Optical power allocation for adaptive WDM transmissions in free space optical networks. In: Proceedings of IEEE Wireless Communications and Networking Conference (WCNC). 2014, 2677–2682
11. Ghassemlooy Z, Popoola W O, Rajbhandari S. Optical Wireless Communications: System and Channel Modelling with MATLAB. Boca Raton, FL: CRC Press, 2012
12. Andrews L C, Phillips R L. Laser Beam Propagation Through Random Media. Bellingham, WA: SPIE Press, 2005, Vol. 52
13. Aladeloba A O, Phillips A J, Woolfson M S. Improved bit error rate evaluation for optically pre-amplified free-space optical communication systems in turbulent atmosphere. IET Optoelectronics, 2012, 6(1): 26–33
14. Motlagh A C, Ahmadi V, Ghassemlooy Z, Abedi K. The effect of atmospheric turbulence on the performance of the free space optical communications. In: Proceedings of 6th IEEE International Symposium on Communication Systems, Networks and Digital Signal Processing (CNSDSP). 2008, 540–543
15. Zhu X M, Kahn J M. Free-space optical communication through atmospheric turbulence channels. IEEE Transactions on Communications, 2002, 50(8): 1293–1300
16. Bandele O J, Desai P, Woolfson M S, Phillips A J. Saturation in cascaded optical amplifier free-space optical communication systems. IET Optoelectronics, 2016, 10(3): 71–79
17. Trinh P V, Dang N T, Pham A T. Optical amplify-and-forward multihop WDM/FSO for all-optical access networks. In: Proceedings of 9th International Symposium on Communication Systems, Networks & Digital Signal Processing (CSNDSP). 2014, 1106–1111
18. Singh S, Kaler R. Flat-gain L-band Raman-EDFA hybrid optical amplifier for dense wavelength division multiplexed system. IEEE Photonics Technology Letters, 2013, 25(3): 250–252
19. Singh S, Kaler R. Novel optical flat-gain hybrid amplifier for dense wavelength division multiplexed system. IEEE Photonics Technology Letters, 2014, 26(2): 173–176
20. Yiannopoulos K, Sagias N C, Boucouvalas A C. Fade mitigation based on semiconductor optical amplifiers. Journal of Lightwave Technology, 2013, 31(23): 3621–3630
21. Agrawal G P. Fiber-Optic Communication Systems. New York: Wiley, 2012, Vol. 222
22. Ramaswami R, Sivarajan K, Sasaki G. Optical Networks: A Practical Perspective. 3rd Edition. San Francisco, CA: Morgan Kaufmann Publishers Inc., 2009,925.
23. Singh M. Performance analysis of WDM-FSO system under adverse weather conditions. Photonic Network Communications, 2018, 36 (1): 1–10
24. Grover M, Singh P, Kaur P, Madhu C. Multibeam WDM-FSO system: an optimum solution for clear and hazy weather conditions. Wireless Personal Communications, 2017, 97(4): 5783–5795
25. Iyer S, Singh S P. Spectral and power efficiency investigation in single-and multi-line-rate optical wavelength division multiplexed (WDM) networks. Photonic Network Communications, 2017, 33 (1): 39–51
26. Jee R, Chandra S. Performance analysis of WDM-free-space optical transmission system with M-QAM modulation under atmospheric and optical nonlinearities. In: Proceedings of 2015 IEEE International Conference on Microwave, Optical and Communication Engineering (ICMOCE), 2015, 41–44
27. Dayal N, Singh P, Kaur P. Long range cost-effective WDM-FSO system using hybrid optical amplifiers. Wireless Personal Communications, 2017, 97(4): 6055–6067
28. Mbah A M, Walker J G, Phillips A J. Performance evaluation of turbulence-accentuated interchannel crosstalk for hybrid fibre and free-space optical wavelength-division-multiplexing systems using digital pulse-position modulation. IET Optoelectronics, 2016, 10(1): 11–20
29. Majumdar A K. Free-space laser communication performance in the atmospheric channel. Journal of Optical and Fiber Communications Reports, 2005, 2(4): 345–396
30. Navidpour S M, Uysal M, Kavehrad M. BER performance of free-space optical transmission with spatial diversity. IEEE Transactions on Wireless Communications, 2007, 6(8): 2813–2819
31. Abaza M, Mesleh R, Mansour A, Aggoune E H. Spatial diversity for FSO communication systems over atmospheric turbulence channels. In: Proceedings of IEEE Wireless Communications and Networking Conference (WCNC). 2014, 382–387
32. Prat J. Next-Generation FTTH Passive Optical Networks. Barcelona: Springer, 2008

Jeremiah O. Bandele obtained a B.Eng. (Hons.) degree in Electrical and Electronic Engineering from the University of Ado-Ekiti (now known as Ekiti State University, Ado-Ekiti) in 2009. He obtained a M.Sc. degree in Electronic, Communications, and Computer Engineering and a Ph.D. degree in Electrical and Electronic Engineering in 2011 and 2016 respectively, from the

University of Nottingham. He worked as a software engineer at Near Field Solutions, Nottingham from 2016 to 2017 where he developed software applications in various software languages and integrated near field communication tags, beacons, Bluetooth and Bluetooth Low Energy devices with the Android SDK. Since 2018, he has been a Lecturer in the Department of Electrical, Electronics and Computer Engineering at Afe Babalola University. His research interests include free-space optical communication, visible light communication, optical amplification, decision thresholding schemes and BER evaluation.

Malcolm Woolfson graduated in 1978 with a B.Sc. degree in Mathematics and Physics from the University of Bristol. Between 1978 and 1981 he was a research student in the Department of Physics at the University of Warwick, where he worked in the area of surface physics. He was awarded a Ph.D. degree in 1982. Between 1981 and 1983 he was employed as a research assistant in the Department of Physics at the University of Sheffield, where he carried out research into the dynamics of atoms in liquids. In 1983 he joined the Marconi Research Centre in Chelmsford, where he worked in the area of signal and data processing techniques for tracking radar. Since 1987 he has been a Lecturer in Signal Processing in the Department of Electrical and Electronic Engineering at the University of Nottingham. He has been involved in the application of a variety of signal and image processing techniques to various areas of engineering.

Andrew J. Phillips received the B.Sc. degree (Hons.) in Mathematics from the University of Manchester, Manchester, UK, in 1990, the M.Sc. degree in Applied Optics from the University of Salford, Manchester, in 1992, and the Ph.D. degree from Manchester Metropolitan University (MMU) in 1995 for a thesis entitled "Optically amplified pulse position modulation systems." He undertook postdoctoral work at MMU from 1995 to 2000, including work on the SuperPON concept in the EU ACTS-PLANET project, and joined Marconi Communications in 2000. He then held a post at the University of Nottingham, Nottingham, UK, as Lecturer in Photonic Communications Technology from January 2003 to August 2017, leaving to pursue interests away from engineering. His research interests have included optical amplification, optical performance monitoring, passive optical networks, free space optical communication, and BER evaluation.